Microchemical Journal 140 (2018) 105–113

Contents lists available at ScienceDirect

Microchemical Journal

journal homepage: www.elsevier.com/locate/microc

Characterization of a label system formed by large unilamellar vesicles for its potential use in the design of electrochemical biosensors

Marcos E. Farías, M. Alejandra Luna, Ana M. Niebylski, N. Mariano Correa, Patricia G. Molina*

Departamento de Química, Facultad de Ciencias Exactas, Físico-Químicas y Naturales, Universidad Nacional de Río Cuarto, Agencia Postal N° 3, 5800 Río Cuarto, Argentina

ARTICLE INFO

Keywords:
Large unilamellar vesicles
Biosensor
Electrochemical label system
Lyophilization process

ABSTRACT

In this contribution a new electrochemical label system formed by DOPC/palmitic acid/cholesterol/sucrose large unilamellar vesicles (LUVs) with $K_4(Fe(CN)_6)$ encapsulated is described and, characterized by using electrochemical techniques, dynamic light scattering (DLS) and transmission electron microscopy (TEM). Results indicates that incorporation of cholesterol to the membrane promote a meaningful reduction in the loss of the encapsulated electroactive molecu1le. On the other hand, the addition of sucrose allows a successful lyophilization process, and confers stability to the system over long periods of time, remaining unchanged even for ten months after being formed. These properties make this system a very stable label that could be linked to an antibody, antigen or DNA strain; after the specific interaction with the analyte, LUVs rupture can be induced and the electroactive molecule encapsulated can be released and electrochemically detected by using square wave voltammetry. These characteristics make this new system into a signal amplifier that can be used to replace traditional enzyme-labels in electrochemical biosensors design.

1. Introduction

In recent years, vesicles have acquired interest in the development of biosensors as labels, because of its ability to carry different molecules in their aqueous cavity [1–4]. Vesicles are spherical aggregates composed of one or multiple lipid bilayers of surfactants. Most of the molecules that form these aggregates are amphiphilic type with low solubility in water. Dissolved in water, they form bilayer self-assemblies type (membrane) in such manner that the polar zones are oriented outwards (aqueous external region), while the hydrophobic zone makes it towards the interior of the bilayer due to the non-specific interactions of the surfactants. The transformation of bilayer to vesicles is thermodynamically favored when energy is applied to the system by ultrasound or pressure differences. These systems are non-toxic, biodegradable and biocompatible which makes them an excellent alternative in their use as nanocarriers [5,6]. Vesicles have been widely used in detection assays as marker carriers to amplify the detection signal [4,7–11].

In the immunosensors design, the interaction between the capture antibody (immobilized) and the antigen, cannot be directly monitored. For this reason quantification of the analyte requires an extra labelling step where an appropriate compound (label molecule) produces a detectable response (e.g. absorbance, fluorescence, current). The magnitude of which is proportional or inversely proportional to the concentration of the analyte in competitive formats [12]. A large number of label systems used in immunosensors have been developed. Some of them are based on electrochemical substances, [13–16] bioluminescence [17,18], enzymes encapsulated [11], decorated vesicles with Au nanoparticles [19] electrogenerated chemiluminescence [20], to mention some of them. However, these systems have disadvantages related to their physical and chemical instability in aqueous solutions (such as hydrolysis and oxidation of phospholipids, aggregation between vesicles and loss of the encapsulated component) [21].

In this regard, different methods have been investigated for vesicle stabilization, such as lyophilization, freezing, spray drying and supercritical fluid technology [22–24]. Among them, the lyophilization is the main method used to prolong the life of the vesicles. This method consists in the elimination of water in frozen state under vacuum. This process is normally used to dry heat-labile products that cannot be dried at high temperatures.

However, it is known that the lyophilization process can greatly affect the structure of the vesicles [25,26]. The contraction of the bilayers after freezing can damage the membranes, the dehydration can generate the fusion or aggregation of vesicles, and a phase transition can occur when the system is rehydrated [27]. Currently, in order to avoid these problems, various lyoprotectants, such as carbohydrates,

* Corresponding author.
E-mail addresses: mfarias@exa.unrc.edu.ar (M.E. Farías), pmolina@exa.unrc.edu.ar (P.G. Molina).

https://doi.org/10.1016/j.microc.2018.04.013
Received 22 December 2017; Received in revised form 20 March 2018; Accepted 11 April 2018
Available online 13 April 2018

are being used to preserve the system [28,29]. In this sense, different measures have been studied that tend to protect the integrity of the membrane during lyophilization. There are many factors that can be considered in order to avoid membrane damage, such as the selection of lyoprotectants, composition of the lipid bilayer of the vesicle and the protocols of the lyophilization process [30,31].

Many sugars have been used as protectors during the lyophilization process, including monosaccharides, disaccharides, polysaccharides and synthetic saccharides. Disaccharides, particularly trehalose [32] and sucrose [33], are accumulated in a variety of organisms that survive osmotic stress or dehydration for long periods. These are effective in protecting the integrity of the membrane, which makes them good lyoprotective substances during the lyophilization of the vesicles. The lyoprotectant effect has been attributed to the ability of these sugars to replace the water surrounding the bilayers by the interaction with the polar region of the surfactant molecules. On the other hand, the formation of a more rigid layer of the lyoprotectant around the bilayer, with a high viscosity and low mobility, prevents the fusion of vesicles, the phase transition and the rupture of the bilayers by the formation of ice crystals [28]. In addition, many techniques have been used to demonstrate these hypotheses, including differential scanning calorimetry (DSC), nuclear magnetic resonance (NMR), infrared spectroscopy (FTIR), scanning electron microscopy (SEM) and dynamic light scattering (DLS) [34–36]. The protective effect of lyoprotectants on lipid bilayers during lyophilization can be characterized by different parameters such as vesicle size (by DLS) and retention or loss of encapsulated solute [28].

On the other hand, cholesterol is also an essential constituent of membranes, one of its main functions being the modulation of the physicochemical properties of the lipid bilayer, controlling the permeability of the membrane by reducing its fluidity [37–39]. Addition of cholesterol to the vesicles formulation can decrease the rate of solute loss after freezing and thawing the vesicles. The presence of cholesterol reduces interactions between carbon chains of phospholipids, preventing aggregation, or increases the interaction between sugars and phospholipids [40,41]. In a study of cholesterol role in the lipid membrane undergoing the drying process, Ohtake et al. observed that the cholesterol addition could alter the gel-to-crystalline phase transition temperature of the lipid membrane which had been lyophilized using trehalose as protector [36]. On the other hand, vesicles that do not contain cholesterol in their lipid bilayer result being more sensitive to degradation in long-term stability studies compared to those containing cholesterol [42].

Luna et al. [43] determined the permeability of 1,2-dioleoyl-sn-glycero-3-phosphatidylcholine (DOPC) LUVs in the presence of different cholesterol contents, by using the enzymatic hydrolysis of N-benzoyl-L-tyrosine p-nitroanilide catalyzed by α-chymotrypsin. They found that cholesterol decreases dramatically the permeability values of the substrate.

Although the use of large unilamellar vesicles (LUVs) in the electrochemical signal amplification has acquired interest in the last years, there are few studies related to the system characterization, regarding the reproducibility of the encapsulation of electroactive molecules, the possible loss of them by permeation when LUVs are in solution, the stability in time, to mention some important issues. To the best of our knowledge, there are very few studies related to the characterization of this type of label system regarding to the amount of electroactive probe encapsulated from different preparations, and the permeation of the molecule through in the membrane, which allows its usefulness as a label in the development of a biosensor.

In this work a new electrochemical label system formed by DOPC/palmitic acid/cholesterol/sucrose LUVs with $K_4(Fe(CN)_6)$ encapsulated is described and characterized by using electrochemical techniques, DLS and transmission electron microscopy (TEM). This label system allows its lyophilisation which makes it very stable for a long time. These characteristics make this new system into a signal amplifier that can be used as a label in electrochemical biosensors. This label system could be linked to an antibody, antigen or DNA strain, and after the specific interaction with the analyte, LUVs rupture is induced and electroactive molecule is released to be electrochemically detected, venue that we are currently investigating.

2. Experimental section

2.1. Materials and methods

The reagents used for the LUVs synthesis were: dioleoyl phosphatidyl choline (DOPC) from Avanti Polar Lipids, palmitic acid and cholesterol, both with purity grade 99% (Sigma-Aldrich), 1-decanethiol purity grade 98% (Sigma-Aldrich), chloroform RA (ACS) (Anhedra), sucrose (Biopack), and Triton X-100 surfactant (TX-100) (Sigma-Aldrich).

Potassium ferrocyanide ($K_4(Fe(CN)_6)$) (Mallinckrodt), glycine 99% purity (Sigma-Aldrich), hydrochloric acid (HCl) pro-analysis (Biopack), lithium perchlorate ($LiClO_4$) (Frederick Smith Chemical Company), and sulfuric acid (H_2SO_4) 95–98% purity (Cicarelli), were used for electrochemically measurements.

The voltammograms were taken with an AUTOLAB PGSTAT30 potentiostat, controlled by GPES 4.8 software by using cyclic voltammetry (CV), electrochemical impedance spectroscopy (EIS) and square wave voltammetry (SWV). The cyclic voltammograms were obtained at scanning rates between 50 and 100 mV/s. The parameters used in the SWV were: the square wave amplitude (ΔE_{SW}) of 0.05 V, the staircase step height (ΔE_S) of 0.01 V and a frequency (f) of 20 Hz. For all measurements a three electrode cell was used.

The working electrodes used were Au disk (area = 0.126 cm^2). They were polished, sonicated, copiously rinsed with distilled water. With the purpose of obtaining good response the electrodes were cycling several times in the H_2SO_4 0.5 M solutions prior to use. The counter electrode was a Pt foil of large area (2 cm^2). A freshly prepared Ag/AgCl, KCl (3 M) reference electrode was used. In all measurements $LiClO_4$ solutions (0.1 M) and glycine solutions adjusted to pH 2 with HCl were used as supporting electrolytes. The pH values were measured with pH-meter Orion 720A calibrated with different buffer solutions.

The diameter of the vesicles was obtained in a Delsa™ Nano Submicron Particle Size and Zeta Potential dynamic light scattering (DLS) equipment C (A53878) model. The determinations were performed at 25 ± 0.1 °C with a laser of λ = 658 nm and detector at 165°. For each sample the equipment performed 150 readings and yielded 3 average values of diameter and polydispersity. To perform LUVs solution measurements, 3 times ultrapure water was first filtered using Varian Nylon-66 pore size filters 0.46 μm (Sigma-Aldrich) in order to remove any particles that caused error in the measurement, then it was placed in a quartz cell with 1 cm optical path and about 10 μL of LUVs solution was added.

Transmission electron microscopy (TEM) images were taken using a Jeol model 1220 microscope. To carry out this experiment a drop of LUV solution was suspended onto carbon coated copper grid using phosphotungstic acid 0.1% as contrast colorant.

Lyophilization of LUVs was carried out in a Labconco Freezone 6 freeze dryer at −35 °C, under vacuum (10^{-3} mbar).

2.1.1. Preparation of LUVs and procedures

2.1.1.1. LUVs preparation. DOPC LUVs were prepared by using an extrusion method [43]. Scheme 1A shows the different synthesis steps of LUVs. A stock solution was prepared by measuring an amount of

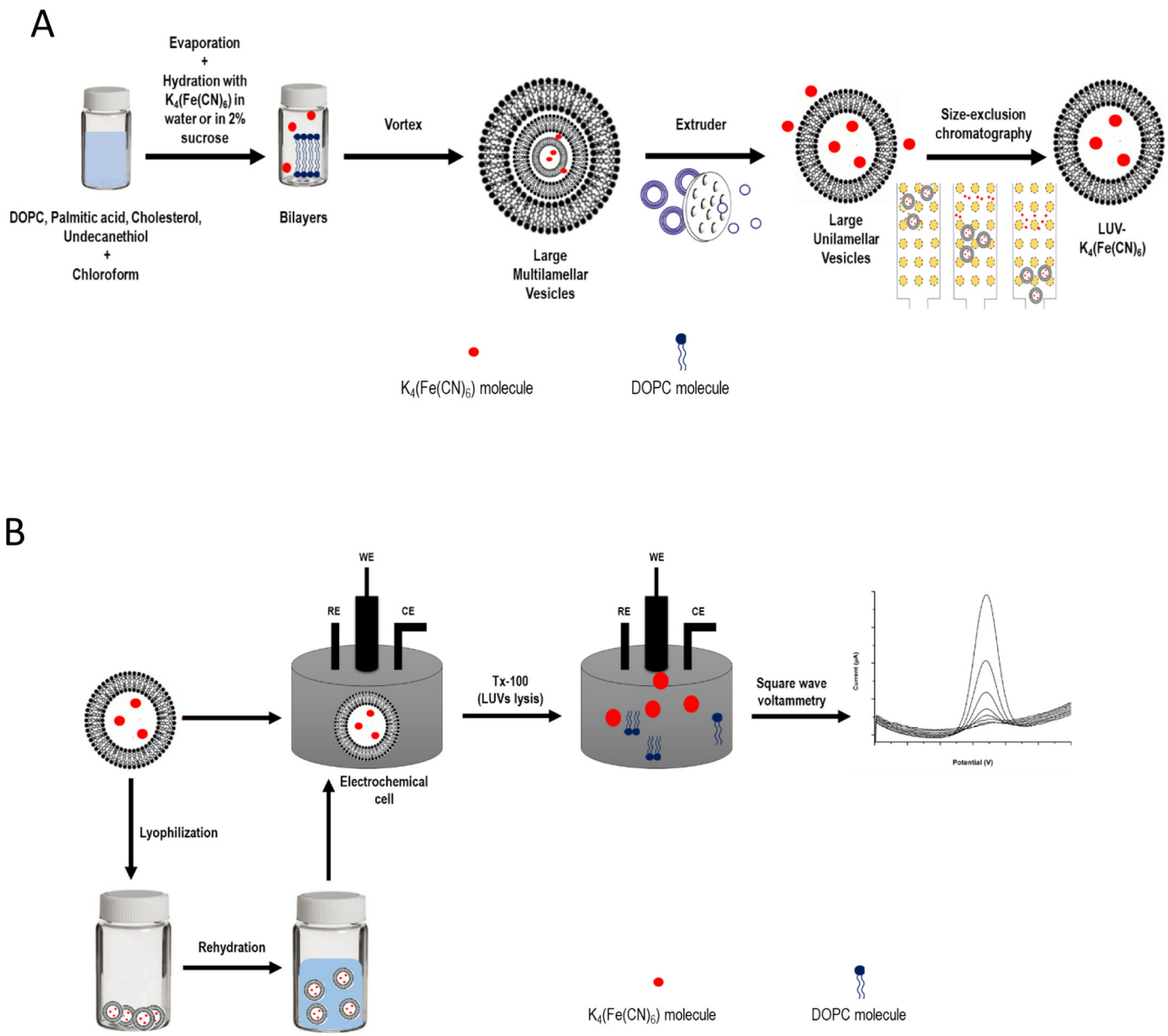

Scheme 1. (A) Squematic illustration of the DOPC/Palmitic acid/Cholesterol/Undecanethiol LUVs formation with $K_4(Fe(CN)_6)$ encapsulated and (B) electrochemical measurement of LUVs and lyophilized LUVs after LUVs rupture.

DOPC (5 mg/mL), palmitic acid (1: 1000 M ratio to DOPC) or cholesterol (0.01 M), or 1-decanethiol (1: 3 M ratio to DOPC) in chloroform according to the experience to be realized. Palmitic acid was added in the appropriate amount to accomplish that every vesicle had, at least one molecule of acid in the bilayer. This incorporation will allow subsequent labelling of different proteins with the vesicle, through the formation of an amide group between the carboxyl group of palmitic acid and the amino terminal of the protein (antibody or DNA) [44]. On the other hand, cholesterol and sucrose were added as lyoprotectants to increase the stability of the bilayer and, to maintain its integrity during the lyophilization and rehydration process. 1-decanethiol was added to proceed with the covalent immobilization of the LUVs on the Au surface. The solutes were dissolved in chloroform and were transferred to a balloon coupled to a rotary evaporator under reduced pressure, where it was dried for 1 h.

After drying the reagent mixture, an aqueous 0.3 M solution of potassium ferrocyanide ($K_4(Fe(CN)_6)$) and/or sucrose solution (2%) was added according to the experience to be realized. The resulting solution was vortexed (Vortex Genie 2) for 5 min at room temperature to promote the formation of multilamellar vesicles (LMVs). LMVs suspension was extruded ten times (Extruder, Lipex biomembranes) through two stacked polycarbonate filters of pore size 200 nm under nitrogen pressure up to 3.4 atm to obtain LUVs solution [43]. After this, free $K_4(Fe(CN)_6)$ (not incorporated in LUVs) was removed by size exclusion chromatography using a sephadex column. To prepare the gel filtration column, we added 2 or 3 g of Sephadex G-50 (Sigma, Aldrich) to 30 mL of ethanol–buffer (4%p/p) solution at 70 °C and we allowed it to swell for 20 min. The LUVs solution was poured into the column (1.0 × 30 cm) and aqueous solution was used as the mobile phase. To the extract obtained from the column, an aqueous solution is added,

until a volume of 1 mL is reached. From this stock solution of LUVs, the different dilutions used in the experimental measurements are prepared.

Finally, LUVs solutions were frozen in vials, with the precaution that solution occupies less than 1/3 of the total volume of the container, to avoid loss of sample during lyophilisation. Later, for comparative purposes, a final volume of 1 mL is reached when rehidrated to obtain the same concentration of lyophilized and non-lyophilized LUVs of the stock solution.

2.1.1.2. Electrochemical measurements. In some experiments, according to the particular aim, electrochemical measurements were carried out immediately after LUVs preparation. In other cases electrochemical detection were realized after of the lyophilisation and subsequent rehydration in an aqueous solution (see Scheme 1B).

For electrochemical measurements, an aliquot of LUVs solution was added to the glycine solution at pH 2 and, square wave voltammograms were performed to determine the peak current (i_p) corresponding to non-altered LUVs with $K_4(Fe(CN)_6)$ encapsulated. Then, TX-100 (8% v/v) was added to the cell containing glycine solution at pH 2 and LUVs with the purpose of provoking the rupture of the LUVs and, the consequent release of $K_4(Fe(CN)_6)$ molecules than can be electrochemically detected. Detection was carried out at different times after LUVs rupture.

For studies referred to find the optimal time of immobilization of LUVs on a surface of gold, an Au disk electrode was used. This electrode was immersed in three aqueous dilutions LUVs with $K_4(Fe(CN)_6)$ encapsulated (1:10, 1:5, 1:2) at different modification times. For each time, Au electrode was removed, rinsed and placed in the electrochemical cell containing an aqueous solution of 1 mM $K_4(Fe(CN)_6)$ in 0.1 M $LiClO_4$, where SWV and electrochemical impedance spectroscopy (EIS) measurements were performed.

For electrochemical measurements of immobilized LUVs on the gold disk, with and without $K_4(Fe(CN)_6)$ encapsulated (labelled and unlabelled, respectively), solutions composed for different quantities of labelled and unlabelled LUVs were previously immobilized on the Au disk during 15 min. Then, the disk was transferred to the electrochemical cell containing 1 mL of glycine solution pH 2. TX-100 was added and after 15 min the SW voltammogram was recorded by using other Au disk electrode for the detection.

3. Results and discussions

3.1. Studies performed with LUVs not immobilized

The electrochemical studies were performed by using SWV. The solution was prepared adding 300 µL of DOPC/palmitic acid/$K_4(Fe(CN)_6)$ encapsulated LUVs solution to final volume of 5 mL pH 2 buffer solution. Fig. 1Ai shows the electrochemical response of LUVs in buffer solution at pH 2. Subsequently, TX-100 is added to this solution in order to produce the rupture of the LUVs, and square wave voltammograms are recorded at different times (Fig. 1ii–vi). After 2 min a signal around 0.2 V that increases with time until reaching maximum value at 15 min can be appreciated. This response would indicate that at this time a complete rupture of LUVs has occurred and all the encapsulated $K_4(Fe(CN)_6)$ has been released. As can be seen, the peak current (i_p) that appears in the Fig. 1Ai is negligible with respect to the one observed after the rupture, indicating that most of $K_4(Fe(CN)_6)$ is encapsulated in the aqueous interior of the LUVs.

In order to verify if the amount of $K_4(Fe(CN)_6)$ encapsulated is similar for different LUVs preparations, SW voltammograms were recorded after addition of TX-100 for ten different LUVs samples. Fig. 1B shows the peak currents obtained in the voltammograms for the different samples. It can be seen that the peak current value practically does not change, so it can be concluded that the preparation process of $K_4(Fe(CN)_6)$ encapsulated in LUVs is highly reproducible so different preparations contain the same amount of electroactive molecule.

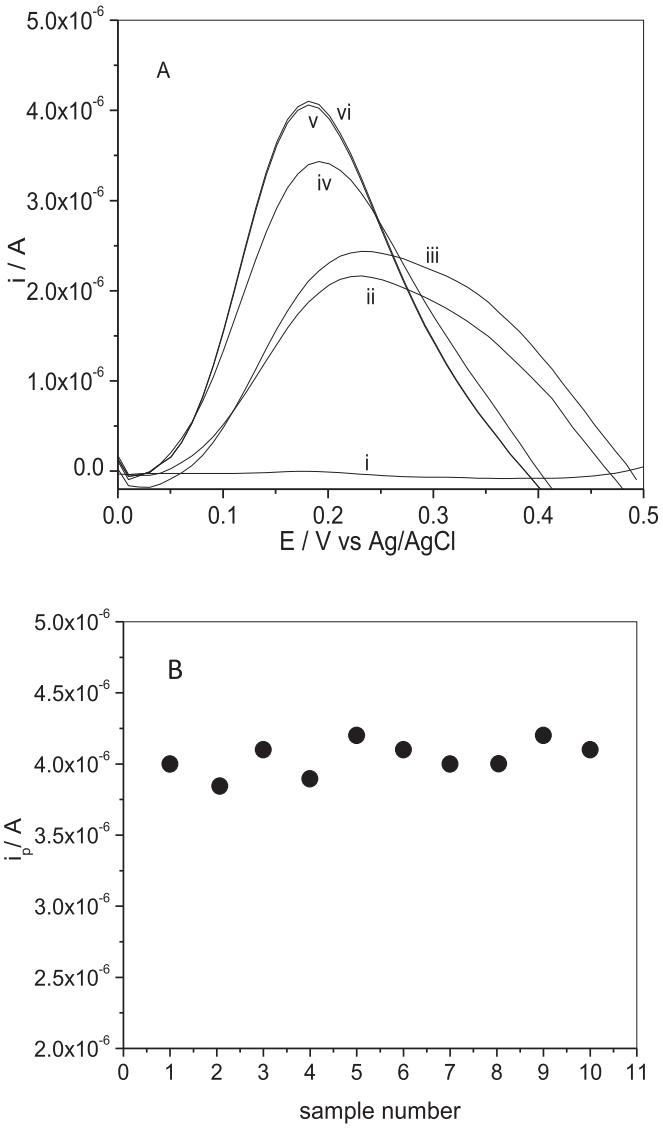

Fig. 1. A) SWV registered when 300 µL of DOPC/palmitic acid/$K_4(Fe(CN)_6)$ encapsulated LUVs stock solution are added to 5 mL final volume of glycine solution pH = 2 before (i) and after LUVs rupture with TX-100 at ii) 2 min, iii) 5 min, iv) 15 min and v) 20 min. B) net peak current SWV obtained for ten samples from different preparations of LUVs after rupture with TX-100. ΔE_{SW} = 0.05 V, ΔE_S = 0.01 V, f = 20 Hz.

3.1.1. Studies of permeability

As discussed previously, one of the disadvantages of these systems is the possibility of losing the encapsulated molecule by permeation through the bilayer over time. Fig. 2A shows recorded voltammograms at different times for a solution containing DOPC/palmitic acid/$K_4(Fe(CN)_6)$ encapsulated LUVs without the addition of TX-100. As can be seen at 60 min (Fig. 2Aii) the peak current corresponding to $K_4(Fe(CN)_6)$ discharge appears due to the loss of the electroactive compound from inside the LUVs to the external aqueous phase. This signal increases with time (Fig. 2Aiii–iv). Fig. 2B shows the percentage loss of

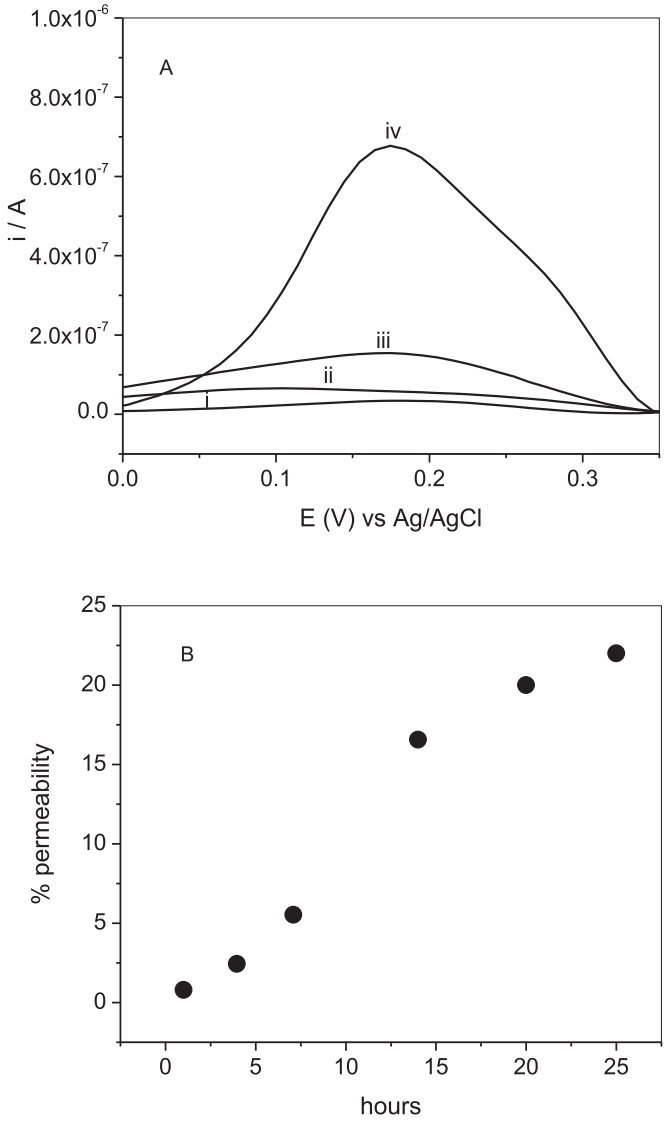

Fig. 2. A) SWV registered with the time, for 300 μL of DOPC/palmitic acid/$K_4(CN)_6Fe$ encapsulated LUVs stock solution added to 5 mL final volume of glycine solution pH = 2 without the addition of TX-100. i) 0 h ii) 1 h, iii) 7 h, iv) 14 h. B) Percentage loss of $K_4(Fe(CN)_6)$ encapsulated over time. ΔE_{SW} = 0.05 V, ΔE_S = 0.01 V, f = 20 Hz.

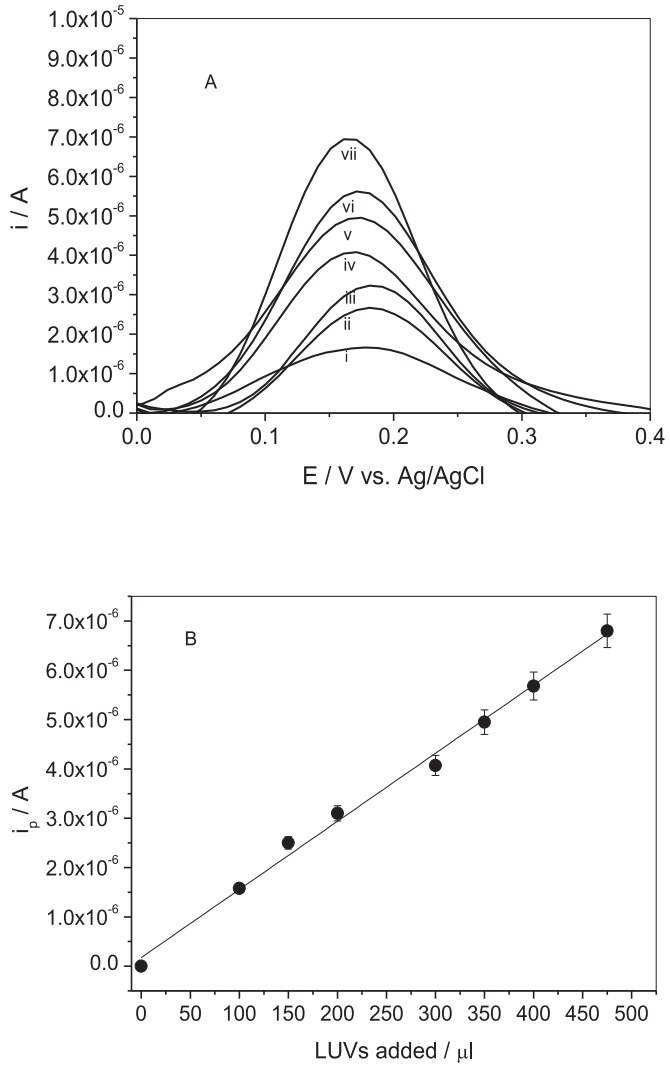

Fig. 3. A) SWV for different aliquots of DOPC/palmitic acid/cholesterol/$K_4(Fe(CN)_6)$ LUVs stock solution added to different aqueous solution of glycine pH 2 with a final volume of 5 mL, after rupture with TX-100. i) 100 μL, ii) 150 μL, iii) 200 μL, iv) 300 μL, v) 350 μL, vi) 400 μL, vi) 475 μL. B) Dependence of i_p on quantity of LUVs. ΔE_{SW} = 0.05 V, ΔE_S = 0.01 V, f = 20 Hz.

$K_4(Fe(CN)_6)$ over time which, at 22 h reaches the value of 22%. Based on these results, we decided to incorporate cholesterol in the LUVs formulation in order to reduce the membrane fluidity [37] and consequently the permeability of electroactive molecule. Besides, previous work has reported that DOPC vesicles containing cholesterol are less permeable to certain substrates, compared with those containing only DOPC [43,45]. Fig. 3A shows the SW voltammograms obtained when different dilutions of LUVs, containing cholesterol, are prepared and, then proceeds to break them. Fig. 3B shows a plot of i_p vs LUVs volume (μL) obtained from the SW voltammograms shown in Fig. 3A, where the i_p is proportional to the volume of LUVs added. Parameters of the linear regression analysis were: slope = $(1.38 \pm 0.04) \times 10^{-8}$ A μL^{-1}; intercept = $(1.2 \pm 0.5) \times 10^{-7}$ A and correlation coefficient, r = 0.993. The results obtained with containing cholesterol LUVs, showed that until 8 h there was no loss of $K_4(Fe(CN)_6)$, after this time a progressive loss of the electroactive molecule is observed, and at 48 h it reaches a loss of 15%.

3.1.2. Studies of stability

3.1.2.1. DLS and TEM measurements. Taking into account the obtained results and considering the potential application of this system for biosensors design, the possibility of lyophilize the vesicles and rehydrate them before their use was also studied with the purpose of increase durability of the system once formed. It is well known that lyophilization processes allow different samples to remain unchanged for months [32,33]. Sucrose was incorporated into the preparation of LUVs, with the aim of protect the integrity of the membrane during the lyophilization process. Then, once they were rehydrated in aqueous solution, LUVs were characterized by different techniques such as DLS and TEM. The sizes were determined by DLS before and after lyophilization at different rehydration times. Table 1 shows the results obtained in each experiment. As can be observed, immediately after rehydration the sizes are larger than those obtained for non-lyophilized LUVs, probably because lyophilized LUVs may undergo some aggregation process. Subsequently, over time, the sizes of the vesicles decrease until reaching a similar size to non-lyophilized LUVs, after 12 h. It should be noted that the size of LUVs lyophilized for

Table 1
Determination of hydrodynamic diameter (Dh) of DOPC/palmitic acid/cholesterol/sucrose/$K_4(Fe(CN)_6)$ encapsulated lyophilized LUVs by using DLS measurements at different experimental conditions.

Procedure	Dh (nm)	Polydispersity
LUVs without lyophilized	193 ± 1	0.1
Lyophilized LUVs and measured immediately after rehydration	381 ± 1	0.2
Lyophilized LUVs and measured 6 h after rehydration	233 ± 4	0.2
Lyophilized LUVs and measured 12 h after rehydration	197 ± 2	0.1
10 months lyophilized LUVs and measured 12 h after rehydration	190 ± 2	0.1

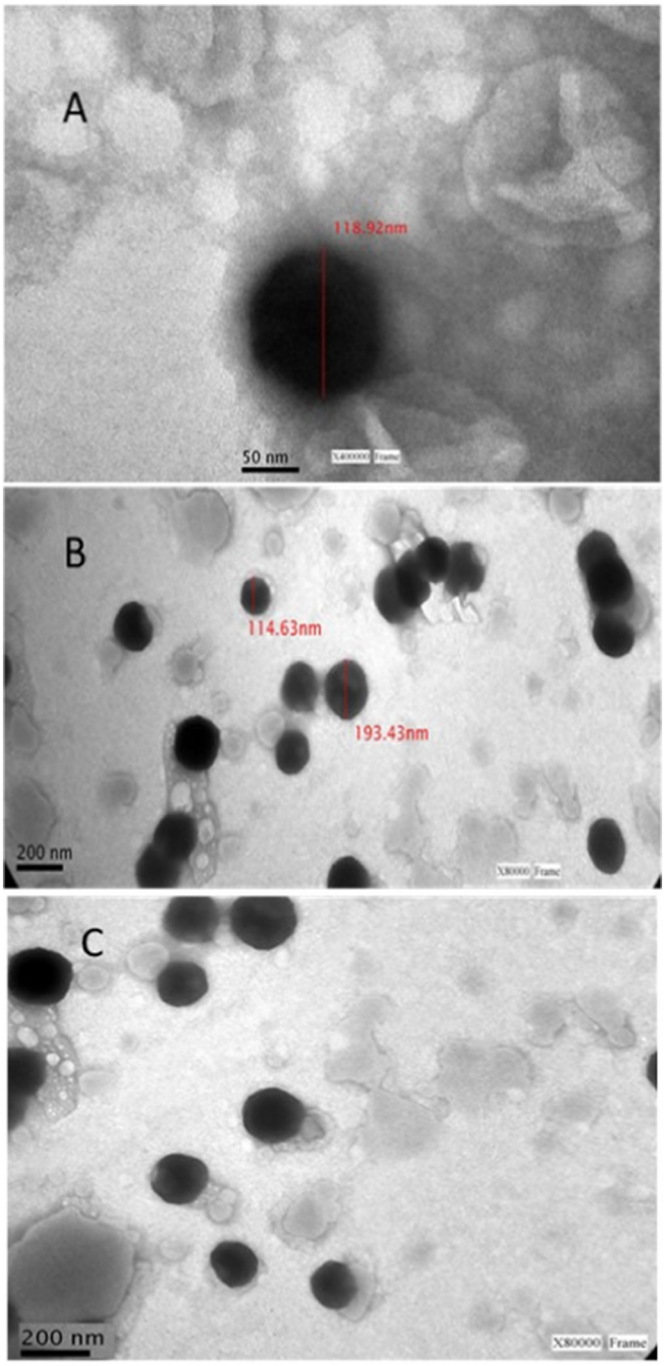

Fig. 4. TEM images taken for LUVs of DOPC/palmitic acid/cholesterol/sucrose/$K_4(Fe(CN)_6)$ encapsulated. (a) LUVs without lyophilization (b) LUVs lyophilized and rehydrated for 2 h (c) LUVs lyophilized and rehydrated for 12 h.

10 months and then rehydrated for 12 h does not change (see the last row of Table 1), which shows the increase in stability of the lyophilised vesicles.

Fig. 4 shows the TEM images for LUVs without lyophilization (Fig. 4A), lyophilized LUVs after 2 h (Fig. 4B) and at 12 h of rehydration (Fig. 4C). As can be seen, in Fig. 4B shows a larger dispersion of sizes and aggregation of LUVs. But, after 12 h (Fig. 4C), the aggregation are no longer observed. The images corroborate the results obtained by DLS.

3.1.2.2. Electrochemical measurements. Electrochemical measurements were performed using lyophilized LUVs composed of DOPC/palmitic acid/cholesterol/sucrose/$K_4(Fe(CN)_6)$ encapsulated and rehydrated 12 h prior to electrochemical experiments. Fig. 5A shows the electrochemical response for different concentrations of rehydrated lyophilized LUVs after the rupture with TX-100. From these voltammograms the i_p values were obtained. Fig. 5B shows a graph of i_p vs volume (μL) LUVs added. As can be observed, the peak current increases linearly with the amount of LUVs added. Parameters of the

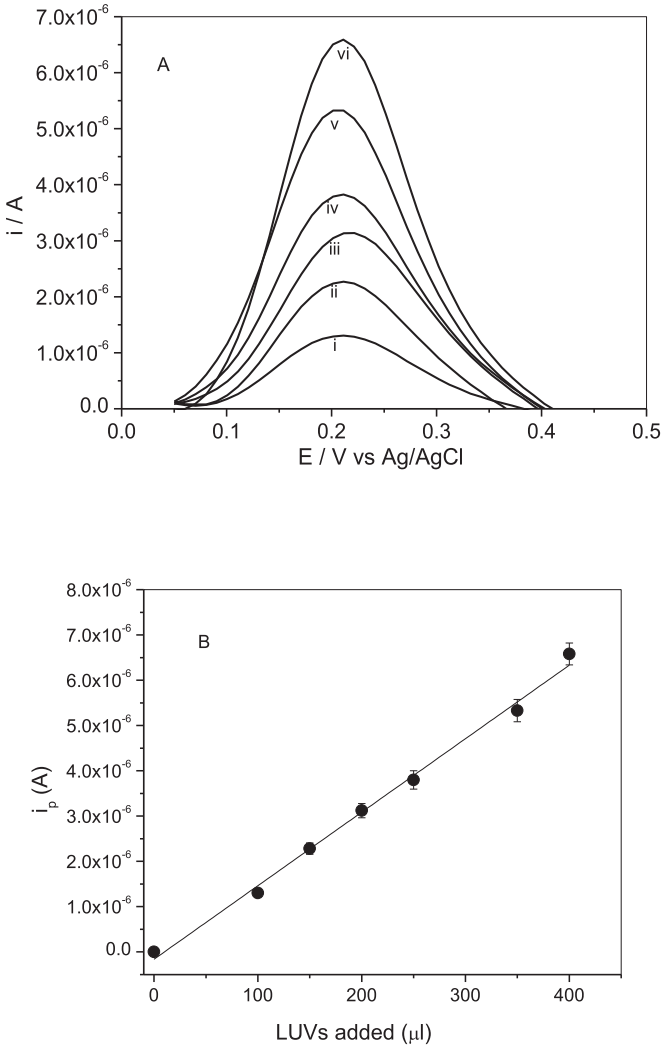

Fig. 5. A) SWV for different solutions prepared from different aliquots of DOPC/palmitic acid/cholesterol/sucrose/$K_4(Fe(CN)_6)$ lyophilized LUVs after 12 h of rehydration and subsequent rupture with TX-100, in glycine pH 2. i) 100 μL, ii) 150 μL, iii) 200 μL, iv) 250 μL, v) 350 μL, vi) 400 μL. B) Dependence of i_p on quantity of LUVs. ΔE_{SW} = 0.05 V, ΔE_S = 0.01 V, f = 20 Hz. The different solutions are taken to a final volume of 5 mL with solution of glycine pH 2.

linear regression analysis were: slope = (1.62 ± 0.04) × 10^{-8} A μL^{-1}; intercept = (−1.5 ± 0.5) × 10^{-7} A and correlation coefficient, r = 0.993. Similar electrochemical studies were performed with 10 months lyophilized LUVs and the variation in the i_p value detected after rupture was found to be less than 5%. These results are very promising for the use of these LUVs as labels for electrochemical biosensors, besides that their response and stability is the same over long periods of time. These characteristics make this particular system a very useful tool for the design of electrochemical sensors.

3.2. Studies of LUVs immobilized on the gold surface

In the design of biosensor the label system is usually linked to the antigen (immunosensor) or DNA strand (genosensor) and it is immobilized on a surface [46–48]. Because our vesicles are proposed for biosensor designs, it is mandatory to evaluate the electrochemical behaviour when LUVs are immobilized on a surface. For this reason, LUVs with $K_4(Fe(CN)_6)$ encapsulated were immobilized on a gold disk surface in order to study its electrochemical response after the rupture.

For the studies performed with LUVs immobilized on the gold surface, 1-decanethiol was added to the bilayer (see Experimental section). It is well known that the thiols adsorb spontaneously on the gold surface to form very stable bonds [49]. First, in order to find the optimum time at which the surface of the gold disk is covered with the immobilized LUVs, the adsorption of LUVs onto gold electrode surface was studied over time. For this purpose, the Au disk was used and immersed in an aqueous solution of LUVs for different time periods. The disk was then removed, rinsed and placed in the electrochemical cell containing an aqueous solution of $K_4(Fe(CN)_6)$ in 0.1 M $LiClO_4$ and, where the SWV and EIS measurements were carried out. Fig. 6A shows the peak current by using modified electrodes at different times for three LUVs solutions (1:10, 1:5, and 1:2 of thiol:DOPC). It can be seen that the peak current decreases with modification time. This decrease in current is due to the fact that the modified electrode surface disrupts the charge transfer of the $K_4(Fe(CN)_6)$ in solution, which is due to the presence of adsorbed LUVs, and depends on the modification time. For the most diluted LUVs solution (Fig. 6Ai) the current does not reach the plateau until 40 min of modification, while for concentrated LUVs solutions the current value becomes constant at 15 min of modification. For practical purposes, it was chosen for further modifications to use a solution of 1:5 thiol:-DOPC. In addition, the modification of the gold surface is also followed by electrochemical impedance spectroscopy (EIS).

Fig. 6B shows a Nyquist plot (Z″ = imaginary impedance part, Z′ = real impedance part) [50]. According to the results shown in Fig. 6B, the charge transfer resistance (Rct) measured by EIS strongly correlates with the processes occurring at the electrode surface. In EIS technique, the semicircle of the plot defines Rct of the redox reaction while, the straight line represents charge diffusion at the electrode surface based on the Randles equivalent circuit. Interestingly, the Rct value increases considerably after the accumulation of LUVs at the surface over time. This indicates that, the gradual modification of the surface inhibits the access of the electroactive molecules to the electrode surface acting as a barrier. From 15 min of modification the semicircles are equals, which indicates that longer times of modification does not change surface coverage and these results are in agreement with those obtained in Fig. 6Aii. Therefore, a modification time of 15 min is chosen.

Then, the electrode was modified with different ratios of the stock solutions of LUVs, with $K_4(Fe(CN)_6)$ encapsulated (labelled) and LUVs without $K_4(Fe(CN)_6)$ (unlabelled) during 15 min. This procedure was performed to simulate a competitive format between labelled and unlabelled molecules. The modified gold disk was then rinsed and taken to the electrochemical cell where voltammograms were recorded after the rupture of the immobilized LUVs with TX-100. A gold auxiliary working electrode was used for these measurements post-rupture. The respective voltammograms are shown in Fig. 7A. As can be seen, the current values increases as the labelled vesicles adsorbed on the surface increases. Fig. 7B shows that the peak current obtained from the voltammograms shown in Fig. 7A, have a linear dependence up to 90% of $K_4(CN)_6$Fe-labelled LUVs. Parameters of the linear regression analysis were: slope = (8.1 ± 0.1) × 10^{-8} A μL^{-1}; intercept = (−6.0 ± 0.1) × 10^{-8} A and correlation coefficient, r = 0.997. These results confirm that this system can be used as a label in the design of electrochemical biosensors.

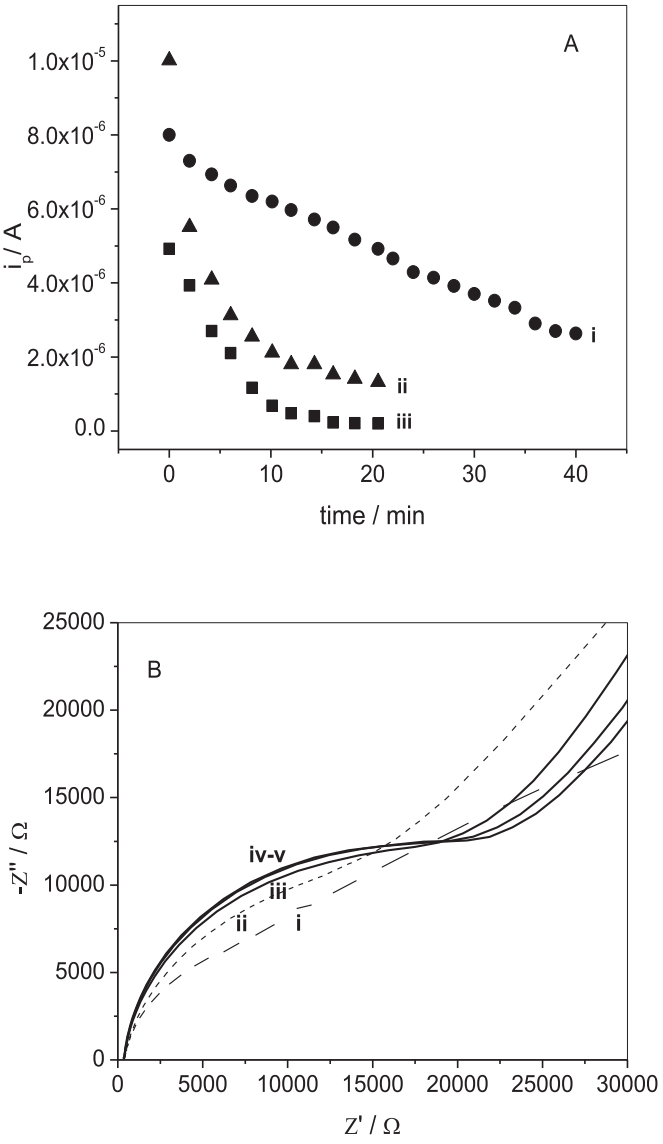

Fig. 6. A) Dependence of the i_p with the time of modification of the electrode with three thiol:DOPC ratio for DOPC/palmitic acid/cholesterol/sucrose/1-decanethiol/$K_4(Fe(CN)_6)$ DOPC LUVs: 1:10 i), 1:5 ii) 1:2 iii). ΔE_{SW} = 0.05 V, ΔE_S = 0.01 V, f = 20 Hz. B) EIS spectra for bare Au i), and modified electrode with DOPC/palmitic acid/cholesterol/sucrose/1-decanethiol/$K_4(Fe(CN)_6)$ DOPC LUVs at ii) 5 min, iii) 10 min, iv) 15 min, v) 20 min. AC amplitude: 5 mV; frequency range: 0.1 Hz to 100 KHz. The work potential is 0.18 V. SW voltammograms and EIS spectres were recorded in a solution of $K_4(Fe(CN)_6)$ in 0.1 M $LiClO_4$ M.

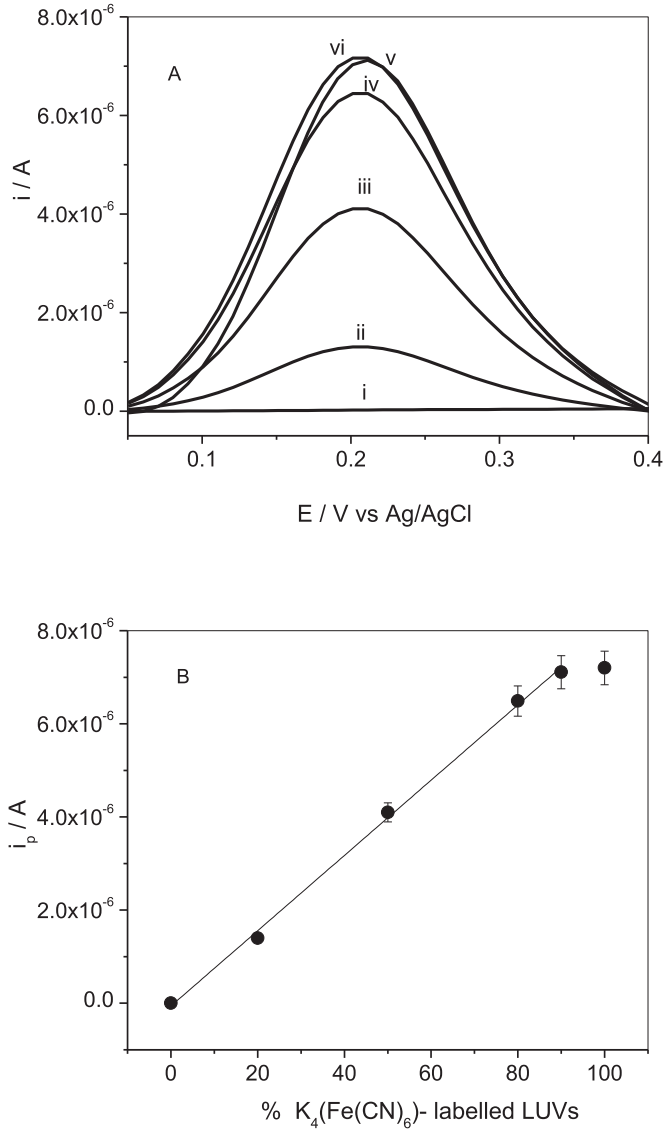

Fig. 7. A) SWV for Au modified electrodes with different LUVs ratios, with (labelled) and without (unlabelled) $K_4(Fe(CN)_6)$ encapsulated LUVs after rupture with TX-100 in solution of glycine pH 2. i) unlabelled LUVs and ii) 20%, iii) 50%, iv) 80%, v) 90%, vi) 100% labelled LUVs. Modification time: 15 min. B) Dependence of i_p on percentage of labelled LUVs. $\Delta E_{SW} = 0.05$ V, $\Delta E_S = 0.01$ V, f = 20 Hz. Volume = 1 mL.

4. Conclusions

In this work we characterized a new electrochemical label system formed by DOPC/palmitic acid/cholesterol/sucrose LUVs with $K_4(Fe(CN)_6)$ encapsulated by using electrochemical techniques, DLS and transmission electron microscopy (TEM).

The composition of this system allowed a successful lyophilization process, which shows electrochemical signals proportional to the quantity of encapsulated electroactive molecule. In addition, the system presents a stability even up to ten months after being prepared, which results in an advantage over other labels.

Additionally, immobilization of label system on a gold surface was optimized. The results show that, after rupture, current signal is proportional to encapsulated electroactive molecule of labelled LUVs, when both (labelled and not labelled) LUVs are adsorbed. This is an important issue, that makes this system appropriated for its use as an effective signal amplifier in electrochemical biosensor design of competitive type format and an attractive tool to replace traditional enzyme-labels in analytical research.

Acknowledgment

Financial support from the Consejo Nacional de Investigaciones Científicas y Técnicas (PIP CONICET 112-201101-00204, PIP CONICET 112-2015-0100283), Universidad Nacional de Río Cuarto (PPI-UNRC 2016-2018), Agencia Nacional de Promoción Científica y Técnica (PICT 2012-0232, PICT 2015-0585 and PICT-2015-2151), and Ministerio de Ciencia y Tecnología, gobierno de la provincia de Córdoba (PID 2013) is gratefully acknowledged. NMC, and PGM hold a research position at CONICET. ML thanks to CONICET for her postdoctoral research fellowship. MEF thanks CONICET for a research fellowship

References

[1] R. Genç, D. Murphy, A. Fragoso, M. Ortiz, C.K. O'Sullivan, Signal-enhancing thermosensitive liposomes for highly sensitive immunosensor development, Anal. Chem. 83 (2011) 563–570.
[2] K.A. Edwards, A.J. Baeumner, Liposomes in analyses, Talanta 68 (2006) 1421–1431.
[3] Y. Zhao, D. Du, Y. Lin, Glucose encapsulating liposome for signal amplification for quantitative detection of biomarkers with glucometer readout, Biosens. Bioelectron. 72 (2015) 348–354.
[4] M. Alizadeh-Ghodsi, A. Zavari-Nematabad, H. Hamishehkar, A. Akbarzadeh, T. Mahmoudi-Badiki, F. Zarghami, M.P. Moghaddam, E. Alipour, N. Zarghami, Design and development of PCR-free highly sensitive electrochemical assay for detection of telomerase activity using nano-based (liposomal) signal amplification platform, Biosens. Bioelectron. 80 (2016) 426–432.
[5] P. Yingchoncharoen, D.S. Kalinowski, D.R. Richardson, Lipid-based drug delivery systems in cancer therapy: what is available and what is yet to come, Pharmacol. Rev. 68 (2016) 701–787.
[6] T.M. Allen, P.R. Cullis, Liposomal drug delivery systems: from concept to clinical applications, Adv. Drug Deliv. Rev. 65 (2013) 36–48.
[7] K.A. Edwards, Y. Wang, A.J. Baeumner, Aptamer sandwich assays: human α-thrombin detection using liposome enhancement, Anal. Bioanal. Chem. 398 (2010) 2645–2654.
[8] T. Takeuchi, S. Matile, DNA aptamers as analyte-responsive cation transporters in fluorogenic vesicles: signal amplification by supramolecular polymerization, J. Am. Chem. Soc. 131 (2009) 18048–18049.
[9] Q. Liu, B.J. Boyd, Liposomes in biosensors, Analyst 138 (2013) 391–409.
[10] M. Kumar, D. Blaas, Human rhinovirus subviral. A particle binds to lipid membranes over a twofold axis of icosahedral symmetry, J. Virol. 87 (20) (2013) 11309–11312.
[11] B. Qu, L. Guo, X. Chu, D. Wu, G. Shen, R. Yu, An electrochemical immunosensor based on enzyme-encapsulated liposomes and biocatalytic metal deposition, Anal. Chim. Acta 663 (2010) 147–152.
[12] W. Ma, D. Li, T.C. Sutherland, Y. Li, Y. Long, H. Chen, Reversible redox of NADH and NAD^+ at a hybrid lipid bilayer membrane using ubiquinone, J. Am. Chem. Soc. 133 (2011) 12366–12369.
[13] W. Liao, J.A. Ho, Attomole DNA electrochemical sensor for the detection of *Escherichia coli* O157, Anal. Chem. 81 (2009) 2470–2476.
[14] S. Viswanathan, L. Wu, M. Huang, J.A. Ho, Electrochemical immunosensor for cholera toxin using liposomes and poly(3,4-ethylenedioxythiophene)-coated carbon nanotubes, Anal. Chem. 78 (2006) 1115–1121.
[15] S. Viswanathana, C. Ranib, C. Delerue-Matos, Ultrasensitive detection of ovarian cancer marker using immunoliposomes and gold nanoelectrodes, Anal. Chim. Acta 726 (2012) 79–84.
[16] J.A. Ho, J. Chiu, J. Hong, C. Ling, K. Hwang, J.R. Hwu, Gold-nanostructured immunosensor for the electrochemical sensing of biotin based on liposomal competitive assay, J. Nanosci. Nanotechnol. 9 (2009) 2324–2329.
[17] J.A. Ho, M. Huang, Application of a liposomal bioluminescent label in the development of a flow injection immunoanalytical system, Anal. Chem. 77 (11) (2005) 3431–3436.
[18] J.A. Ho, C.H. Hung, Using liposomal fluorescent biolabels to develop an immunoaffinity chromatographic biosensing system for biotin, Anal. Chem. 80 (2008) 6405–6409.
[19] M.F. Barroso, M.A. Luna, J.S. Flores Tabares, C. Delerue-Matos, N.M. Correa, F. Moyano, P.G. Molina, Gold nanoparticles covalently assembled onto vesicle structures as possible biosensing platform, Beilstein J. Nanotechnol. 7 (2016) 655–663.
[20] W. Zhan, A.J. Bard, Electrogenerated chemiluminescence. 83. Immunoassay of human C-reactive protein by using $Ru(bpy)_3^{2+}$-encapsulated liposomes as labels,

Anal. Chem. 79 (2007) 459–463.
[21] V.P. Torchilin, V. Weissig, Liposomes: A Practical Approach, 2nd ed, Oxford Univ. Press, New York, 2003.
[22] K. Mishima, Biodegradable particle formation for drug and gene delivery using supercritical fluid and dense gas, Adv. Drug Deliv. Rev. 60 (2008) 411–432.
[23] Y.L. Lo, J.C. Tsai, J.H. Kuo, Liposomes and disaccharides as carriers in spray-dried powder formulations of superoxide dismutase, J. Control. Release 94 (2004) 259–272.
[24] U.S. Kadimi, D.R. Balasubramanian, U.R. Ganni, M. Balaraman, V. Govindarajulu, In vitro studies on liposomal amphotericin B obtained by supercritical carbón dioxide-mediated process, Nanomedicine 3 (2007) 273–280.
[25] R. Benjakul, B. Panyarachun, N. Sarisuta, Preparation of dry reconstituted liposomal powder by freeze-drying at room temperature, J. Liposome Res. 21 (2011) 28–37.
[26] B. Stark, G. Pabst, R. Prassl, Long-term stability of sterically stabilized liposomes by freezing and freeze-drying: effects of cryoprotectants on structure, Eur. J. Pharm. Sci. 41 (2010) 546–555.
[27] P. Wessman, K. Edwards, D. Mahlin, Structural effects caused by spray and freeze-drying of liposomes and bilayer disks, J. Pharm. Sci. 99 (2010) 2032–2048.
[28] L.M. Crowe, C. Womersley, J.H. Crowe, D. Reid, L. Appel, A. Rudolph, Prevention of fusion and leakage in freeze-dried liposomes by carbohydrates, Biochim. Biophys. Acta 861 (1986) 131–140.
[29] T.D. Madden, M.B. Bally, M.J. Hope, P.R. Cullis, H.P. Schieren, A.S. Janoff, Protection of large unilamellar vesicles by trehalose during dehydration: retention of vesicle contents, Biochim. Biophys. Acta 817 (1985) 67–74.
[30] C. Chen, D. Han, C. Cai, X. Tang, An overview of liposome lyophilization and its future potential, J. Control. Release 142 (2010) 299–311.
[31] T. Toniazzo, S.C. Pinho, Lyophilized Liposomes for Food Applications: Fundamentals, Processes, and Potential Applications. Encapsulation and Controlled Release Technologies in Food Systems, 2nd ed, John Wiley & Sons, Ltd. (Eds), Chichester, UK, 2016, pp. 78–96.
[32] J. Swaminathan, C. Ehrhardt, Effect of lyophilization on liposomal encapsulation of salmon calcitonin, J. Liposome Research 24 (2014) 297–303.
[33] V. Kannan, P. Balabathula, L.A. Thoma, G.C. Wood, Effect of sucrose as a lyoprotectant on the integrity of paclitaxel-loaded liposomes during lyophilisation, J. Liposome Research 25 (2015) 270–278.
[34] G. Strauss, P. Schurtenberger, H. Hauser, The interaction of saccharides with lipid bilayer vesicles: stabilization during freeze–thawing and freeze–drying, Biochim. Biophys. Acta 858 (1986) 169–180.
[35] C. Cacela, D.K. Hincha, Low amounts of sucrose are sufficient to depress the phase transition temperature of dry phosphatidylcholine, but not for lyoprotection of liposomes, Biophys. J. 90 (2006) 2831–2842.
[36] W.C. Mobley, H. Schreier, Phase transition temperature reduction and glass formation in dehydroprotected lyophilized liposomes, J. Control. Release 31 (1994) 73–87.
[37] H. Ohvo-Rekila, B. Ramstedt, P. Leppimaki, J.P. Slotte, Cholesterol interactions with phospholipids in membranes, Prog. Lipid Res. 41 (2002) 66–97.
[38] Y. Barenholz, Cholesterol and other membrane active sterols: from membrane evolution to “rafts”, Prog. Lipid Res. 41 (2002) 1–5.
[39] V. Monje-Galvan, J.B. Klauda, Two sterols, two bilayers: insights on membrane structure from molecular dynamics, Mol. Simul. 1 (2017) 1–10.
[40] A.V. Popova, D.K. Hincha, Effects of cholesterol on dry bilayers: interactions between phosphatidylcholine unsaturation and glycolipid or free sugar, Biophys. J. 93 (2007) 1204–1214.
[41] S. Ohtake, C. Schebor, J.J. de Pablo, Effects of trehalose on the phase behavior of DPPC–cholesterol unilamellar vesicles, Biochim. Biophys. Acta 1758 (2006) 65–73.
[42] A.M. Samuni, A. Lipman, Y. Barenholz, Damage to liposomal lipids: protection by antioxidants and cholesterol-mediated dehydration, Chem. Phys. Lipids 105 (2000) 121–134.
[43] M.A. Luna, J.J. Silber, L. Sereno, N.M. Correa, F. Moyano, Determining the substrate permeability through the bilayer of large unilamellar vesicles of DOPC. A kinetic study, RSC Adv. 6 (2016) 62594–62601.
[44] Y. B-Wan, W. Deng, Y. Su, X. Zhu, C. Peng, H. Hu, H. Peng, S. Song, C. Fan, Carbon nanotube-based ultrasensitive multiplexing electrochemical immunosensor for cancer biomarkers, Biosens. Bioelectron. 30 (2011) 93–99.
[45] Z. Cui, M. Lafleur, Lamellar self-assemblies of single-chain amphiphiles and sterols and their derived liposomes: distinct compositions and distinct properties, Colloids Surf. B 114 (2014) 177–185.
[46] M.J. Monerris, F.J. Arevalo, H. Fernandez, M.A. Zón, P.G. Molina, Integrated electrochemical immunosensor with gold nanoparticles for the determination of progesterone, Sensors Actuators B Chem. 166–167 (2012) 586–592.
[47] Y. Wan, Y. Su, X. Zhu, G. Liu, C. Fan, Development of electrochemical immunosensors towards point of care diagnostics, Biosens. Bioelectron. 47 (2013) 1–11.
[48] P.A. Rasheed, N. Sandhyarani, Carbon nanostructures as immobilization platform for DNA: a review on current progress in electrochemical DNA sensors, Biosens. Bioelectron. 97 (2017) 226–237.
[49] D. Nassoko, M. Seydou, C. Goldmann, C. Chanéac, C. Sanchez, D. Portehault, F. Tielens, Rationalizing the formation of binary mixed thiol self-assembled monolayers, Mater. Today Chem. 5 (2017) 34–42.
[50] G. Valincius, M. Mickevicius, T. Penkauskas, M. Jankunec, Electrochemical impedance spectroscopy of tethered bilayer membranes: an effect of heterogeneous distribution of defects in membranes, Electrochim. Acta 222 (2016) 904–913.